

Ge(100) 2×1 and $c(4 \times 2)$ surface reconstructions studied by *ab initio* total-energy molecular-force calculations

L. Spiess*

Commissariat à l'Energie Atomique, Service de Recherche sur les Surfaces et l'Irradiation de la Matière,
Bâtiment 462, Centre d'Etudes de Saclay, 91191 Gif-sur-Yvette Cedex, France
and Département de Physique, Université de Paris-Sud, 91405 Orsay Cedex, France

A. J. Freeman

Department of Physics and Astronomy, Northwestern University, Evanston, Illinois 60208-3112

P. Soukiassian

Commissariat à l'Energie Atomique, Service de Recherche sur les Surfaces et l'Irradiation de la Matière,
Bâtiment 462, Centre d'Etudes de Saclay, 91191 Gif-sur-Yvette Cedex, France
and Département de Physique, Université de Paris-Sud, 91405 Orsay Cedex, France

(Received 17 June 1993)

The 2×1 and $c(4 \times 2)$ surface reconstructions on Ge(100) are investigated by the *ab initio*, all-electron, molecular-cluster method, which solves the local-density-functional equations and provides analytical energy gradients. We use finite-size clusters (up to 71 atoms including 39 Ge atoms) to model the Ge(100) surfaces. Atomic-force calculations are extensively used to obtain the minimum-energy geometry for the different structures investigated. We determine and compare the binding energy and geometry up to the fourth layer of the symmetric (2×1), buckled (2×1), as well as the higher-order $c(4 \times 2)$ reconstruction. Important energetic and structural differences are found compared to the corresponding Si(100) 2×1 surface. The asymmetric dimer model is found to be 0.34 eV/dimer lower than the symmetric one with the up-dimer atom being 0.19 Å above the plane of the unreconstructed surface and a dimer tilt of 15°. The buckled 2×1 and $c(4 \times 2)$ reconstructions are found to be close in energy, which suggests that both could be present on the surface at room temperature. These results are in excellent agreement with scanning-tunneling-microscopy experiments and previous theoretical studies using a slab geometry. This energy is well below the energy of the symmetric dimer reconstruction indicating that dimer flipping recently suggested for the Si(100) 2×1 surface is unlikely to occur in the case of the Ge(100) surface. In significant contrast to the Si(100) surface, we found that the Ge-Ge dimer is weaker with bond lengths that are slightly above the bulk value of 2.44 Å, at 2.48 and 2.50 Å for the asymmetric 2×1 and $c(4 \times 2)$ reconstructions, respectively. It suggests that the Ge(100) surface might show some different behavior towards adsorption.

I. INTRODUCTION

Due to fundamental and applied interests, the structure of clean and adsorbate covered group-IV semiconductor surfaces has been widely investigated theoretically and experimentally in recent years,^{1,2} especially for silicon.³⁻⁵ The surface structures of germanium, another important group-IV semiconductor, were much less investigated.⁶⁻⁹ Despite rather similar electronic properties, the Ge surfaces exhibit some puzzling differences when compared to those for silicon, especially in their interaction with adsorbates.¹⁰⁻¹³ In view of this, a good knowledge of the surface structure on the atomic scale is essential for the comprehensive understanding of the general properties of Ge surfaces. The reconstructions of the Ge(100) surface have been investigated recently using various models,¹⁴⁻¹⁸ which were primarily used for experimental data interpretation. So far, there was only one *ab initio* theoretical study of the Ge(100) surface, in

which a pseudopotential approach with a slab geometry was used.^{8,9} Another possible approach is the *ab initio* molecular-cluster DMol method using finite-size clusters. Since it does not use crystal translational symmetry, it is very suitable to study local effects such as reconstructions and some may be used for both clean and adsorbed surfaces. Since this method has been successfully applied in semiconductor surface and interface studies,^{5,19-21} it is suitable for the investigation of the Ge(100) 2×1 surface and its higher-order reconstructions.

It is now well established that both Ge(100) 2×1 and Si(100) 2×1 surfaces reconstruct with dimer formation.²² A key issue concerns the symmetric or asymmetric nature of the dimer. Although many experimental and theoretical works have favored the asymmetric dimer for the Si(100) 2×1 surface, a recent *ab initio* DMol investigation has shown that both symmetric and asymmetric dimers may coexist on the surface.⁵ Now, scanning tunneling microscopy (STM) is a unique tool for the direct

observation of dimers as shown, for example, for the Ge(100) 2×1 surface by Kubby *et al.*⁶ Interestingly, recent STM studies have shown the existence on the same Si(100) 2×1 surface of both symmetric and asymmetric dimers,^{23–25} which are found to be in equal amount in the study by Tromp, Hamers, and Demuth.²³ In addition, buckling of Si-Si dimers was observed to occur mainly near step edges and/or defects,^{24,25} while asymmetric (buckled) dimer stabilization by defects was supported by a recent theoretical work.²⁶ It is also possible that surface preparation, especially the annealing temperature, might play an important role in the existence of symmetric and/or asymmetric Si-Si dimers.²⁵ A recent model based on dynamical flipping of asymmetric dimers was also proposed to explain the observation of time-averaged symmetric dimers in STM topographic images.^{27,28}

So far, there is less debate concerning the nature of the Ge-Ge dimers for the Ge(100) 2×1 surface. Both experiment^{6,29,30} and theory^{7–9} have favored the asymmetric dimer model; similarly, some investigations have favored the asymmetric dimer model by comparing theoretical calculations and experimental data.^{14–18} Exceptions include a work based on the simple Keating model³¹ and a structural model proposed to interpret core-level results of clean and halogen-covered Ge(100) 2×1 .³² One should remark that, in the case of symmetric Ge-Ge dimers, the only possible reconstruction for the Ge(100) surface is 2×1 . However, the situation is different in the case of the asymmetric dimer model where, in addition to the buckled $b(2\times 1)$, higher-order Ge(100) reconstructions such as $c(4\times 2)$ or $p(2\times 2)$ can be observed as a result of the different possible arrangements of the buckled dimers (see Fig. 1). These higher-order reconstructions are ex-

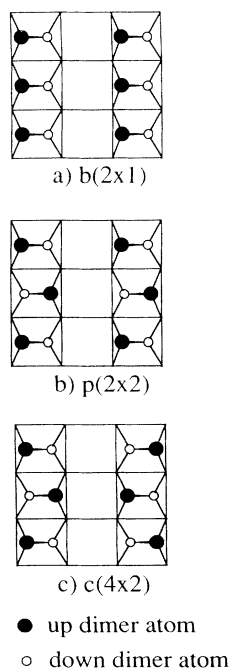


FIG. 1. Schematic top view of the different arrangements of asymmetric dimers on the Ge(100) surface [(a) buckled $b(2\times 1)$] and high-order reconstructions [(b) primitive $p(2\times 2)$ and (c) centered $c(4\times 2)$].

pected to be close in energy³³ because the dimer-dimer interaction which derives this longer-range ordering is weaker in energy than the driving force of the dimer bond formation (by one order of magnitude).⁶ The accepted picture of the reconstructed Ge(100) surface is that of an asymmetric dimer ordering in a 2×1 structure at room temperature (RT), while at low temperature (LT), the surface reconstructs with a $c(4\times 2)$ arrangement.³⁴ A phase transition was predicted³³ to occur between the 2×1 and $c(4\times 2)$ structures and observed^{29,34,35} in the temperature range from 200 to 250 K.

In contrast, Kubby *et al.*⁶ observed domains at RT with local $p(2\times 2)$ and $c(4\times 2)$ symmetries in high-resolution STM images of the Ge(100) surface. Using He diffraction, Lambert *et al.*¹⁴ also observed an additional $c(4\times 2)$ structure at RT and a residual contribution from an apparent 2×2 component at LT. In addition, Needels, Payne, and Joannopoulos,^{8,9} in their *ab initio* pseudopotential calculations, found the $c(4\times 2)$ and $p(2\times 2)$ reconstructions almost degenerate and about 0.07 eV per dimer lower than the $b(2\times 1)$. They also suggested the existence of a phase transition at 380 ± 100 K, between the ordered $c(4\times 2)$ or $p(2\times 2)$ state and the disordered $b(2\times 1)$ state, in further support of the existence of higher-order reconstructions at RT.⁹

In this article, we present a detailed investigation of the Ge(100) surface reconstructions using *ab initio*, self-consistent total-energy molecular-cluster DMol calculations.³⁶ We model the surface with finite-size clusters and compare the different reconstructions arising from surface dimerization. We find that the buckled 2×1 and $c(4\times 2)$ reconstructions are close in energy, well below the energy of the symmetric 2×1 reconstruction, indicating that the dimer flipping model recently suggested for the Si(100) 2×1 surface is unlikely to occur in the case of the Ge(100) surface. In significant contrast to the Si(100) 2×1 surface, the Ge asymmetric dimer is weaker with bond lengths slightly larger than the bulk value, which could result in some changes in the surface response towards adsorbates when compared to silicon. We also find some other important structure differences with the corresponding Si(100) 2×1 surface. In the next section, we describe briefly the method and the details of our calculation. In Sec. III we present and discuss the results for the three reconstructions investigated, and conclusions are presented in Sec. IV.

II. METHOD AND COMPUTATIONAL DETAILS

The DMol all-electron total-energy method³⁶ solves the local-density-functional equations and provides analytical energy gradients,³⁷ which enable force calculation and geometry optimization.³⁸ The method was described earlier and successfully applied to the investigation of Si(100) 2×1 surface reconstruction⁵ and interface structures such as alkali metals^{19,20} and Sb (Ref. 21) on Si(100) 2×1 , as well as various other systems.^{39–41} In all these works^{5,19–21} and in the present one, the investigated surface and interface is modeled by finite-size clusters. The Hedin-Lundqvist exchange-correlation potential was used.⁴² Cluster size and geometry are determined accord-

ing to the properties that are investigated. Here, since we calculated the optimized reconstructed geometry of the Ge(100) 2×1 surface using the force calculation procedure implemented in the DMol method, we need to have an accurate representation of both the dimer atoms and the second- to fourth subsurface layers. Previous DMol calculations performed on the Si(100) 2×1 structure⁵ have shown the optimal cluster size that allows a reliable study of the relaxation of the atoms without perturbations due to vacuum boundary effects.

To study first the reconstruction of the symmetric dimer Ge(100) 2×1 surface, we have used the two clusters Ge31-H28 and Ge39-H32, shown in Figs. 2(a) and 2(b), respectively. Choosing two different clusters to study the reconstruction of the surface allows us to avoid the use of a very large cluster embedding all inequivalent atoms of the unit cell in its center. The first cluster allows a good description of the structural and electronic properties of the dimers [atoms 1 and 1' in Fig. 2(a)] and the second- to fourth-layer Ge atoms under the dimers (atoms 2, 2', 3, and 4). In order to avoid edge boundary effects, only center atoms of the cluster are used to obtain structural results (see Fig. 2). Therefore we have built a second cluster to represent the third and fourth layers in the valley between two dimers (atoms 3' and 4' in Fig. 2). Moreover, in addition to providing the reconstruction geometry of atoms 3' and 4', the cluster in Fig. 2(b) enables double checking of the optimized geometry of layers 1 and 2 determined with the cluster in Fig. 2(a). It should be reminded that, in cluster calculations, the cluster size is important because of the system artificial boundary with the vacuum. For the Ge covalent semiconductor, we are confident that the surface can be represented with our clusters, but the reconstruction effects are modeled within the accuracy of these clusters.

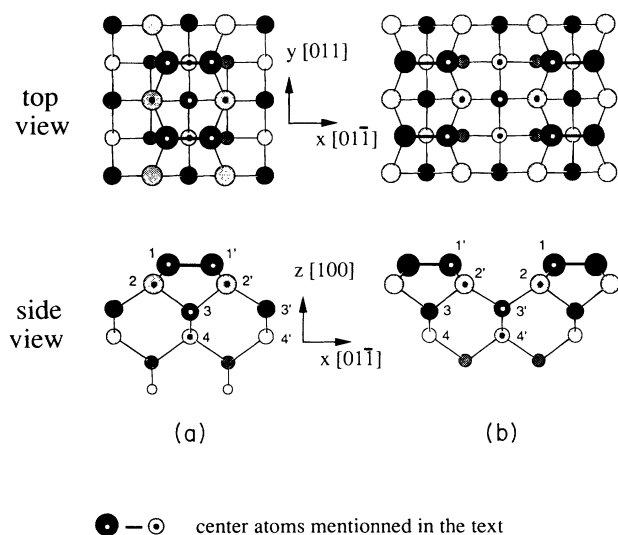


FIG. 2. Clusters used for the investigation of the symmetric dimer reconstructed Ge(100) 2×1 surface. "Center atoms" used in the geometry optimization (step 1) are represented with a dot. (a) Ge31-H28 and (b) Ge39-H32. Hydrogen atoms are not represented for clarity.

For both clusters, we restricted the calculations to geometries that preserve C_{2v} symmetry, which enables block diagonalization of the Hamiltonian matrix.

For the asymmetric dimer reconstructions, since we investigated higher-order geometries together with the 2×1 surface, we performed preliminary calculations on 21 and 31 Ge atom clusters [see Figs. 3(a) and 3(b)] and refined our results on a large cluster Ge31-H28 [Fig. 3(c)], which is the same as the cluster in Fig. 2(a), but without the C_{2v} symmetry restriction. We did not impose any symmetry restrictions on the clusters in Fig. 3 in order to test and compare different asymmetric dimer configurations, thus keeping all degrees of freedom for the investigation of symmetry breaking. The computational effort is roughly increased by a factor of 4 when compared to the symmetric dimer investigation. For example, the three-dimensional mesh partitioning the numerical integrations for the cluster in Fig. 3(c) is increased to 132 000 points and the size of the matrix files exceeds 1 Gbyte.

In order to saturate the dangling bonds of the subsurface boundary Ge atoms, we used the hydrogen embedding scheme which was successfully applied to Si clusters. The Ge dangling bonds (except for those of the surface dimer Ge atoms) are replaced by a Ge-H bond of 1.53 Å—the sum of covalent radii—which yields similar properties to the Ge-Ge bond. In this work, we used for

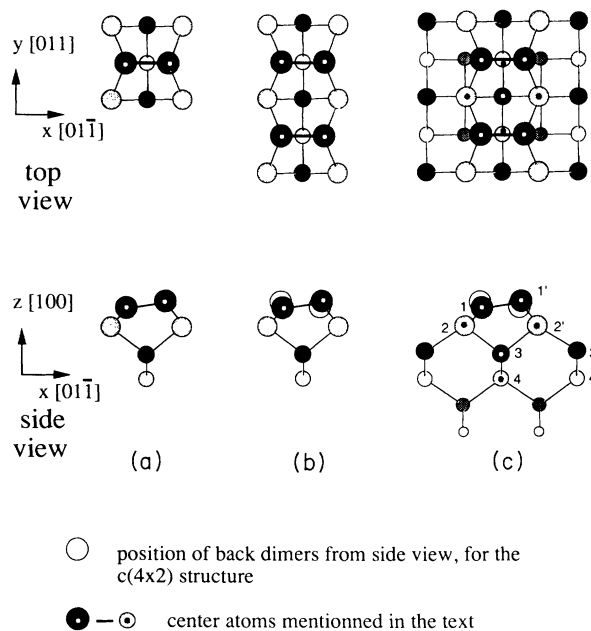


FIG. 3. Clusters used for the investigation of the asymmetric dimer reconstructed Ge(100) surface. Center atoms used in the geometry optimization (step 1) are represented with a dot. (a) Ge9-H12, (b) Ge15-H16, and (c) Ge31-H28. Hydrogen atoms are not represented for clarity. Clusters (b) and (c) are used to study both the $b(2 \times 1)$ symmetry with parallel dimers and the $c(4 \times 2)$ reconstruction with alternating dimers as shown in the side view with empty spheres for the projection of background dimers. The small clusters (a) and (b) provide only qualitative results, useful in the investigation of cluster (c).

all final results a DND basis that consists of one set of core orbitals, a double set of valence orbitals ($4s, 4s', 4p, 4p'$), and a polarization function of $4d$ type. The frozen-core approximation was used up to the $3p$ orbitals. The resulting energy levels and molecular orbital occupations show that, although taken into the calculation, the full $3d$ shell is not affected and remains in the core. A double numerical basis was used for the hydrogen atoms. Calculations on the clusters in Figs. 3(a) and 3(b) were done with a reduced basis, without the d -polarization function, in order to investigate many configurations and check for local minima at lower computational cost.

The binding energy of a cluster is defined as $E_b = E_t - E_a$, where E_t is the total energy of the cluster and E_a is the sum of each atomic energy. For a given atomic geometry, the binding energy of the system and the forces on each atom are calculated. The degree of convergence is measured by root-mean-square changes in the charge density and is set to 10^{-5} Ry for the total energy. The force convergence criterion is 3.0×10^{-3} Ry/a.u. unless otherwise specified. To find the optimized geometry, the atoms involved are further displaced according to the forces acting on them. An optimized geometry is obtained when all the forces are sufficiently small. As will be further seen, particular attention was brought to the determination of the force convergence criterion in order to obtain the energy minimum for a given geometry optimization. The degrees of freedom for the reconstruction are x and z coordinates for first- and second-layer Ge and a z coordinate for the third- and fourth-layer Ge. It was verified for the asymmetric (2×1) dimer model that y coordinate displacements along the $[011]$ direction of first- and second-layer Ge atoms increased the forces acting on them and are thus unlikely to happen. On the other hand, similar displacements for the second-layer atoms of the $c(4 \times 2)$ structure were taken into account for the optimized structure.

III. RESULTS AND DISCUSSION

Since a cluster method is used to study the Ge(100) surface, we give here some details of the hydrogen embedding scheme. As stated, the subsurface Ge dangling bonds are replaced by a Ge-H bond of 1.53 Å. This scheme has several advantages, namely, (i) it keeps the electrons of the subsurface dangling bonds localized in a Ge-H bond similar to the Ge-Ge bond, and thus reduces greatly the boundary effects; (ii) it increases the size of the cluster by one additional "shell" at low computational cost; and (iii) it allows better convergence of the self-consistent procedure, which is usually hard to obtain in the case of highly delocalized systems. The only price one has to pay for such a procedure is a small charge transfer estimated as <0.15 electrons from the bonded boundary Ge to H. For greater reliability, only Ge atoms in the center of the cluster (see Figs. 2 and 3) are used for geometry optimization, i.e., Ge atoms bonded to four other Ge atoms. In order to further check our model, we performed a complementary calculation with the same conditions, but with a larger Ge-H bond length of 1.57

Å.⁴³ Forces on center Ge atoms were found to be strictly the same for both values of the Ge-H bond length and the energy difference between symmetric and asymmetric dimer models was the same to within less than 5×10^{-3} eV. We are therefore confident that our results do not depend on the model chosen.

In Fig. 4 we show a contour plot of the total charge density of the symmetric dimer Ge(100) 2×1 surface, in the plane of the dimers parallel to the surface for the cluster in Fig. 2(b). It can be seen that neither the edge boundary with the vacuum nor the hydrogen bonds induce deformation to the electronic structure of the dimers: the contour plots are similar for the value in the center of the cluster and on both sides. This confirms that the surface structure and electronic properties are not dependent on either the choice of the cluster geometry or the embedding procedure, as long as the cluster is chosen large enough.

A. Symmetric or asymmetric nature of the Ge(100) 2×1 surface dimer

In order to address the nature of the dimer, we have calculated the relative stability and geometry of the Ge(100) 2×1 surface reconstruction with symmetric and asymmetric dimers. The procedure used to carry out the geometry optimization on all clusters can be described by iterations over two steps: (1) we calculated forces on center atoms of the cluster (see Figs. 2 and 3) and further optimize their coordinates while all other atoms are fixed and (2) the geometry of the noncenter atoms (fixed in the first step) was changed to the calculated geometry determined for equivalent center atoms while these center atoms are kept in their optimized position. After completion of the second step, the new electronic structure arising from these coordinate changes creates new forces on the center atoms which must again be optimized. We

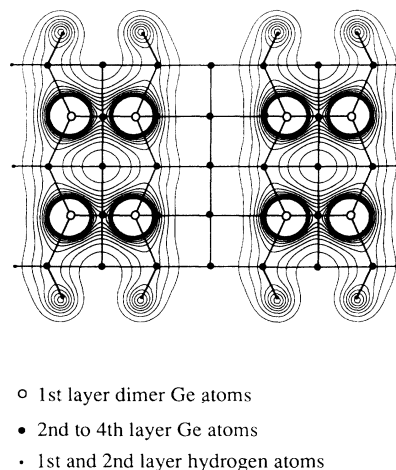


FIG. 4. Contour plot of the total charge density of the symmetric dimer reconstructed Ge(100) 2×1 surface showing the edge boundary with the vacuum and the hydrogen atoms. The plot is done in the (001) plane, parallel to the surface, and passing through the dimers, on the Ge39-H32 cluster [from Fig. 2(b)] using C_{2v} symmetry. Contour spacings are $0.011 e/(\text{a.u.})^3$.

therefore repeated step 1 and did as many needed iterations for convergence of this “geometry pseudo-self-consistent” procedure. This pseudo-self-consistency should not be confused with the self-consistent method itself, which calculates solutions of the Kohn-Sham equations for a given geometry by iterations over the total charge density. “Geometry self-consistency” is attained when the change of coordinates of noncenter atoms in step 2 does not create new significant forces on the center atoms (in our case, two to four iterations were necessary for convergence). This procedure allows the geometry optimization to rely only on those center atoms which are not sensitive to edge boundary effects.

As can be seen for the clusters shown in Fig. 2 for the symmetric dimer reconstruction, all inequivalent atoms of the unit cell lie at least once within the center atoms of either the cluster in Fig. 2(a) or 2(b). Furthermore, it should be noted that the geometry of the first- and second-layer Ge atoms, determined with both clusters in Figs. 2(a) and 2(b) as a double check, were found to be the same within less than 0.01 Å. This confirms that the size of the clusters is very suitable to study the reconstruction of the Ge(100) surface. One should also notice that for the asymmetric dimer model, we did not use another cluster, as for the symmetric case, in order to obtain the optimized coordinates of atoms 3' and 4' which lie on the boundary of the cluster in Fig. 3(c) (see Fig. 3). Although atoms 3' and 4' are not optimized on the cluster in Fig. 3(c), we calculated forces acting on them. These forces did not change between symmetric and asymmetric dimer models and the coordinates of atoms 3' and 4' were therefore kept fixed for the investigation of the asymmetric dimer reconstruction. Small clusters [Figs. 2(a) and 3(b)] were used to obtain quantitative results useful in the investigation of the larger cluster [Fig. 3(c)].

We now look at the coordinates calculated for the 2×1 symmetric and asymmetric reconstructions. In Table I we present the atomic displacements obtained for the four top layers of the Ge(100) surface for all three recon-

structions investigated: symmetric 2×1 , asymmetric $b(2 \times 1)$, and $c(4 \times 2)$. It can be seen that the reconstruction mainly affects the first-layer atoms 1 and 1', which form dimers, while second- to fourth-layer atoms relax by less than 0.10 Å. The symmetric dimer reconstruction was found to be similar to that of the symmetric Si(100) 2×1 surface (see Ref. 2 and references therein): first-layer Ge atoms move towards the bulk and form dimers with a bond length of 2.33 Å, significantly shorter than the bulk bond length at 2.44 Å. When symmetry is broken, one can see in Table I for the asymmetric $b(2 \times 1)$ model the formation of up- and down-dimer atoms. For the asymmetric dimer, it is important to note that the up-dimer atom relaxes above the position of the ideal unreconstructed surface (z coordinate of atom 1' is positive; see Table I). This situation is very different from the case of Si(100) 2×1 where in both cases of symmetric and asymmetric Si dimers, the two Si atoms relax downward.^{4,5} For the Ge asymmetric 2×1 reconstruction, we found the dimer bond length to be 2.48 Å, i.e., 0.15 Å larger than for the symmetric dimer and 0.04 larger than the bulk bond length (2.44 Å). This result shows an important difference compared to Si(100) 2×1 where both symmetric and asymmetric dimer bonds are shorter than the bulk bond length.^{4,5} The Ge dimer bond is therefore significantly weaker in the asymmetric model. This weaker Ge dimer bond length might be responsible for some of the very significant differences observed in surface reactivity and metal-semiconductor interface formation between the Si(100) and Ge(100) surfaces.^{10,12,13}

In Fig. 5, we present contour plots of the total charge density of the symmetric and asymmetric dimers in a plane perpendicular to the surface. As mentioned above, one can see in Fig. 5(b) a large displacement of the up-dimer Ge atom compared to its position in the symmetric dimer [Fig. 5(a)]. Moreover, for the asymmetric dimer, the back bond $D_{1'2'}$ between up-dimer atom 1' and atom 2' is stretched to 2.53 Å while the D_{12} back bond between down-dimer atom 1 and atom 2 is equal to the bulk bond

TABLE I. Ideal coordinates (X, Y) and calculated atomic displacements ($\Delta X, \Delta Y$) of the four top layers of the Ge(100) surface with symmetric 2×1 , asymmetric $b(2 \times 1)$, and $c(4 \times 2)$ reconstructions on the Ge31-H28 cluster [Figs. 2(a) and 3(c)]. Dimer bond lengths are also computed. All distances are in angstroms.

	Ideal surface		Symmetric 2×1		Asymmetric 2×1		$c(4 \times 2)^b$	
	X	Z	ΔX	ΔZ	ΔX	ΔZ	ΔX	ΔZ
1	-1.994	0.000	0.830	-0.241	1.126	-0.463	1.105	-0.468
1'	1.994	0.000	-0.830	-0.241	-0.474	0.187	-0.469	0.198
2	-1.994	-1.409	0.073	0.054	0.036	0.060	0.062	0.068
2'	1.994	-1.409	-0.073	0.054	-0.089	0.078	-0.062	0.068
3	0.000	-2.818	0.000 ^a	-0.090	0.000 ^a	-0.085	0.000 ^a	-0.085
3'	3.998	-2.818	0.000 ^a	0.092	0.000 ^a	0.092	0.000 ^a	0.092
4	0.000	-4.227	0.000 ^a	-0.037	0.000 ^a	-0.029	0.000 ^a	-0.029
4'	3.998	-4.227	0.000 ^a	0.000	0.000 ^a	0.000	0.000 ^a	0.000
R_D			2.33		2.48		2.50	

^aNot included as a degree of freedom in the geometry optimization.

^bFor the $c(4 \times 2)$ reconstruction only, atoms 2 and 2' have a ΔY shift of 0.074 and -0.074 Å, respectively. They both move away from the down-dimer atom and towards the up-dimer atom.

length (2.44 Å). Both back bonds on the symmetric dimer are slightly compressed at 2.41 Å. By inspecting the contours between the two atoms of the Ge dimer (Fig. 5), one can see that there is less charge for the asymmetric dimer than for the symmetric one, i.e., 60×10^{-3} and $76 \times 10^{-3} e/(a.u.)^3$, respectively. In order to compare our results for the Ge(100) surface with the corresponding contour plot obtained for the symmetric and asymmetric dimers of the Si(100) 2×1 surface (Fig. 3 of Ref. 5), we have used the same contour spacing, $4 \times 10^{-3} e/(a.u.)^3$. The contour spacings in Ref. 5 indicate the same amount of charge between atoms of both symmetric and asymmetric dimers on the Si(100) 2×1 surface at $88 \times 10^{-3} e/(a.u.)^3$. This is consistent with the value of both Si dimer bond lengths, which were found to be

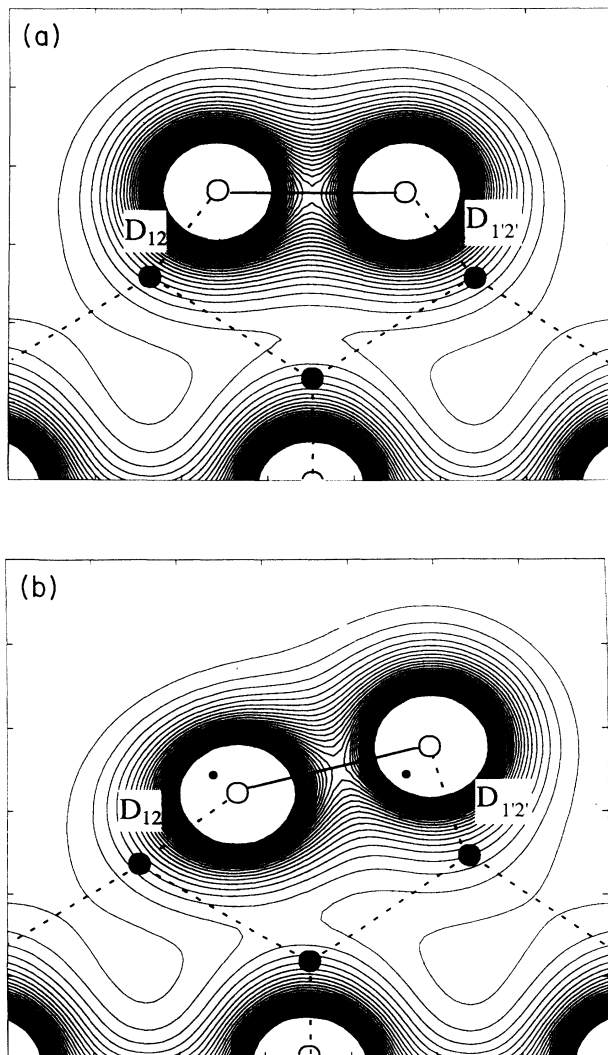


FIG. 5. Contour plot of the total charge density of the Ge(100) 2×1 surface for (a) symmetric dimer and (b) the asymmetric dimer (positions of symmetric dimer atoms are recalled by small dots). The plots are in the (011) plane passing through the dimers and cutting the surface at a right angle. Contour spacings are $0.004 e/(a.u.)^3$. Solid circles represent out-of-plane Ge atoms.

shorter than the Si bulk bond length⁵ and further stresses that the dimer bond in Si is stronger than in the Ge dimer for both symmetric and asymmetric cases.

We now consider the results obtained for the subsurface layers of Ge(100). For the asymmetric 2×1 model, the second-layer atoms move only slightly to compensate the bond stretchings arising from the asymmetry of the dimers; the third- and fourth-layer atoms are almost unaffected by the asymmetry. This seems to indicate an important screening of the electronic structure as well as a smoothing of the bond stretching of surface Ge atoms towards the bulk. It appears also that bond length conservation is not the sole mechanism of the Ge(100) 2×1 reconstruction since the asymmetric Ge dimer exhibits some important strain due to bond stretching. This does not imply that the asymmetric dimer is unstable, since it has a large lowering of the total binding energy (as compared to the symmetric dimer), as will be seen below. Our result indicates that the main structural differences between Ge symmetric and asymmetric models are concentrated in the dimer atoms (see Table I).

Further valuable information can be provided by the binding energies calculated for the three structures investigated with the cluster in Fig. 2(c) (see Table II). From the calculated energies of Table II, it appears that the asymmetric dimer model is more favorable by far than the symmetric one, with a large energy difference of 0.68 eV (or 0.34 eV per dimer), in good agreement with previous work.^{8,15} This large energy difference represents a major contrast between Ge(100) 2×1 and Si(100) 2×1 , which was found to have energy differences as low as 0.02 eV per dimer.⁵ It also suggests that the flipping dimer model, proposed and discussed for the interpretation of STM topographs for Si(100) 2×1 ,^{27,28} is unlikely to occur for Ge(100) 2×1 . In this dynamical process, the intermediate structure between the two equivalent positions of the asymmetric dimer is the symmetric dimer, which has a much higher energy. Furthermore, the consequent calculated activation barrier of 0.34 eV between symmetric and asymmetric dimer models is one order of magnitude larger than the thermal excitation energy at room temperature. Interestingly, Wolkow²⁸ was able to interpret the stabilization of asymmetric dimers on Si(100) by defects on STM topographs at RT and LT in terms of blocking of the dimer flipping, which partially propagated through the dimer row. Also, based on a molecular-dynamics simulation, Weakliem, Smith, and Carter²⁷ pro-

TABLE II. Binding energy E_b calculated for the three investigated reconstructions of the Ge(100) surface on the Ge31-H28 cluster [Figs. 2(a) and 3(c)], with ΔE_b the energy difference (per dimer) with the symmetric 2×1 dimer structure as reference. Note that since the Ge31-H28 cluster contains two dimers, ΔE_b is half the cluster energy difference. All energies are in eV.

Reconstruction	E_b (eV)	ΔE_b /dimer (eV)
symmetric 2×1	-186.63	0
asymmetric 2×1	-187.31	-0.34
$c(4 \times 2)$	-187.34	-0.36

vide an interesting picture of the Si(100) surface with a complex mix of dynamic switching of symmetric and asymmetric dimers. Our interpretation of a rather static Ge(100) surface [as compared to Si(100)2×1] matches very well the recent STM observations, which clearly show that defects are not necessary for the stabilization of Ge asymmetric dimers.⁶

Since the determination of the minimum-energy configuration is based on force optimization, we have checked the influence of the force convergence criterion on the accuracy of both the geometry and the minimum binding energy. In Table III, we show the three steps of the asymmetric dimer structure optimization, starting from the geometry of the optimized symmetric dimer. First, we observed that the symmetric dimer structure is metastable, since a breaking of the dimer symmetry lowers the energy. Then, one can see that, by setting the force convergence criterion to 5×10^{-3} Ry/a.u., one reaches an asymmetric structure that is 0.67 eV lower in energy than the symmetric one. By further optimizing the forces below 3×10^{-3} Ry/a.u., one again lowers the energy (by 0.01 eV) with coordinate changes below 0.01 Å, but with significant additional CPU cost. This shows that 3×10^{-3} Ry/a.u. is a perfectly suitable force convergence criterion and that trying to go beyond it would not yield any further insight. However, one can easily see the importance of the force convergence criterion determination: its contribution to the error made on the calculated energy should be evaluated and taken into account. This further stresses that one should be especially careful when building an interpretation with small energy differences.

We now present some complementary information obtained with the smaller clusters in Figs. 3(a) and 3(b). Note that these results are more qualitative since the Ge basis set used is smaller and that relaxation is restricted to first-layer dimer atoms. Although the size of the clusters in Figs. 3(a) and 3(b) is not sufficient to model the surface up to the fourth layer, it is perfectly suitable to study the behavior of the first-layer dimer atoms. For both asymmetric 2×1 and c(4×2) reconstructions, we have verified that the optimized geometry found on the cluster in Fig. 3(c) was not a local energy minimum. Moreover, we also checked different starting geometries for each reconstruction. We then calculated the energy differences between the symmetric and asymmetric dimer

and found 0.25 and 0.30 eV per dimer on the clusters in Figs. 3(a) and 3(b), respectively. These energies are comparable since they were calculated under the same conditions with the same geometry for the dimer atoms. Knowing that the cluster in Fig. 3(a) has only one dimer, while the cluster in Fig. 3(b) has two, the additional 0.05 eV lowering of the asymmetric dimer binding energy can be roughly attributed to the dimer-dimer interaction. This result lead us to study the total energy of the different reconstructions on a cluster that embeds two dimers, so that we can account for this dimer-dimer interaction. The other information one can obtain is the contribution of second-layer relaxation to the energy lowering between symmetric and asymmetric dimers. Since we found an energy difference of 0.34 eV using the Ge31-H32 cluster [Figs. 2(a) and 3(c)] between symmetric and asymmetric dimers, the additional 0.04 eV per dimer compared to the result with the cluster in Fig. 3(b) may be attributed to relaxation of subsurface layers which were kept fixed on the cluster in Fig. 3(b). An additional result obtained with these small clusters is that the symmetric dimer configuration is on top of an energy curve with respect to tilting of the dimers. Therefore, the symmetric dimer is unstable to infinitesimal breaking of the symmetry, which appears to be different from the Si(100)2×1 surface.

We now compare in Table IV our results for the dimer coordinates of the buckled 2×1 structure with the only two theoretical works providing structural informations as atom coordinates.^{8,15} As we can see in Table IV, there is, in general, good agreement between the three investigations which use different methods. Our calculated dimer bond length at 2.48 Å is in excellent agreement with that of Pollman, Krüger, and Mazur,¹⁵ while Needels, Payne, and Joannopoulos find a shorter one.⁸ Reconstruction of the second and third layers exhibit slight differences, namely, an absolute shift of 0.10–0.15 Å of the z coordinate for all layers, toward the bulk, as compared to the slab geometry calculation.⁸

B. Ge(100)c(4×2) higher-order reconstruction

It now appears clearly from our work and most of the previous ones including both theoretical and experimental investigations^{6–9,14–18,29,30} that the asymmetric dimer model is favored over the symmetric one. Therefore, it is

TABLE III. Intermediate steps (for different values of the force convergence criterion F) in the optimization of the asymmetric 2×1 structure on the Ge31-H28 cluster [Figs. 2(a) and 3(c)]. The optimized symmetric 2×1 structure is chosen as the starting geometry. We show for each step the binding energy E_b of the cluster and its difference ΔE_b with the symmetric structure as energy reference, i.e., for the final optimization, all forces are below 3×10^{-3} Ry/a.u.

Ge ₃₁ -H ₂₈ (two-dimer cluster)	Symmetric dimer	Asymmetric dimer		
		broken symmetry	first optimization	second and final optimization
F (10^{-3} Ry/a.u.)	< 3	< 19	< 5	< 3
E_b (eV)	− 186.63	− 186.94	− 187.30	− 187.31
ΔE_b (eV) per two dimers	0	− 0.31	− 0.67	− 0.68

TABLE IV. Atomic displacements of dimer atoms (1 and 1' in Fig. 3) for the asymmetric $b(2 \times 1)$ reconstruction of the Ge(100) surface. The present calculation is compared with results of Pollman, Krüger, and Mazur (Ref. 15) and Needels, Payne, and Joannopoulos (Ref. 8). The dimer bond length R_D is also given. All distances are in angstroms.

$b(2 \times 1)$	Present work		Ref. 15		Ref. 8 ^a	
	ΔX	ΔZ	ΔX	ΔZ	ΔX	ΔZ
1	1.126	-0.463	1.123	-0.520	1.200	-0.289
1'	-0.474	0.187	-0.462	0.112	-0.418	0.260
R_D	2.48		2.49		2.43	

^aIn order to compare with our results, we have expressed distances in Ref. 8 in the same unit as the present work, assuming a bulk bond length of 2.44 Å.

important to investigate the possible higher-order reconstructions which arise from the different arrangements of asymmetric dimers on the Ge(100) surface (see Fig. 1). The main structural feature of the $c(4 \times 2)$ and $p(2 \times 2)$ reconstructions is the “zig-zag” pattern of the asymmetric dimers in a row, while their main difference is the dimer interaction between adjacent rows as can be seen from Fig. 1. In our *finite-size cluster* investigation, we do not account for the long-range ordering which differentiates these two structures. Therefore, when we investigated the reconstructed $c(4 \times 2)$ structure on the cluster in Fig. 3(c) with alternating dimers, we could not distinguish it from the $p(2 \times 2)$ structure. In the *ab initio* slab geometry study,⁹ two separate calculations were performed for these two reconstructions. However, an energy difference of 0.003 eV was found between the $c(4 \times 2)$ and the $p(2 \times 2)$ structure, which lies within the accuracy of the method. It shows that the long-range dimer interaction is very weak compared to the short-range interaction. This should not change significantly the geometry of the dimers between $c(4 \times 2)$ and $p(2 \times 2)$ reconstructions.

In the case of the $c(4 \times 2)$ structure, as one can see from Table I, the geometry of the dimer atoms is almost the same as for the asymmetric 2×1 case (except that dimers alternate in a row). The dimer bond length of 2.50 Å is even larger than that of the asymmetric 2×1 structure at 2.48 Å, and so can be interpreted as an even weaker dimer bond. This feature is especially interesting in views of the very peculiar behavior of the Ge(100) surface as compared to the Si(100) one upon adsorbate deposition.^{10,12,13} It suggests that this important difference in the dimer bond lengths between Ge(100) and Si(100) could be of relevance in these cases.

The main differences between $c(4 \times 2)$ and 2×1 reconstructions are the following: the second-layer Ge atoms become symmetric under the $c(4 \times 2)$ reconstruction and undergo relaxation along the [011] direction (Fig. 3).⁸ This comes from the fact that atoms 2 and 2' no longer have a different structural environment as compared to the asymmetric 2×1 structure and become images with respect to a C_2 rotation along a [001] axis passing through the center of the cluster in Fig. 3(c). All second-layer Ge atoms are then bonded to one up- and one down-dimer atom with back bonds of 2.50 and 2.47 Å, respectively. Relaxation of second-layer atoms in the [011] direction leads to reduced stretching of the backbonds as

compared to the $b(2 \times 1)$ reconstruction.^{3,8}

So far, the only available geometry, given by Needels, Payne, and Joannopoulos⁸ for the $c(4 \times 2)$ reconstruction exhibits a breaking of the reflection symmetry of the (011) plane and is therefore rather different from the one proposed here, although the magnitude of the displacements is similar. We have checked for lateral displacements along the y coordinate for atoms on the two top layers and found an increase of both forces and binding energy, thus showing that such a symmetry breaking does not occur. Later, Needels, Payne, and Joannopoulos⁹ found this breaking to be negligible, but did not mention to what extent this correction affected the coordinates they had presented earlier.⁸ Also of interest, Appelbaum and Hamann showed for the Si(100) 2×1 surface that, while dimers can easily relax since their dangling bond is free, second-layer atoms undergo a strong angular strain with respect to bond bending since they are tetracoordinated.³

Within the asymmetric dimer model, we found the $c(4 \times 2)$ structure to be 0.04 eV per dimer lower than the 2×1 asymmetric structure, which is a small energy difference (see Table II). Since the optimization was done with and without the y coordinate degree of freedom for the two top layers, we can safely assign 0.025 eV out of the 0.04 eV per dimer to relaxation of second-layer atoms along the [011] direction. While energy difference is small, it nevertheless exhibits an intrinsic lowering of the energy due to dimer alternation. We propose here a simple explanation, in addition to the already proposed relaxation of second-layer atoms:⁸ as can be seen in Fig. 1, the two alternating $p(2 \times 2)$ and $c(4 \times 2)$ configurations correspond to an optimal space filling, where the distance between up-dimer atoms is maximum and the electronic repulsion is minimized in the case of charge imbalance between up- and down-dimer atoms. This simple picture agrees well with our results, which show a small energy difference between the $c(4 \times 2)$ and 2×1 structures. This argument is in contradiction with a recent interpretation of an x-ray diffraction experiment which finds some relaxation of the surface up to the tenth layer.¹⁷

From our structural and energetic results, we can see that the $c(4 \times 2)$ structure has the lowest energy configuration for the dimer reconstruction of the Ge(100) surface. Needels, Payne, and Joannopoulos⁹ concluded that the degenerate $c(4 \times 2)/p(2 \times 2)$ structure is the ground state of the Ge(100) surface with an energy difference of 0.066 eV per dimer between the 2×1 and

$c(4 \times 2)$ structures. Our present calculations at 0 K show that, with a small energy difference of 0.04 eV per dimer between 2×1 and $c(4 \times 2)$ reconstructions, one is likely to see both on the surface, together with the $p(2 \times 2)$ [which cannot be distinguished from $c(4 \times 2)$ in this work]. In the case of the $c(4 \times 2)$ reconstruction, the second-layer atoms play an important role as we mentioned above. It is possible that with a larger cluster, including several other fully bonded second-layer Ge atoms, we might find a larger energy difference between 2×1 and $c(4 \times 2)$ reconstructions, as is the case in Ref. 9. This would mean that with the actual size of our cluster, the possibility that we might miss part of the relaxation energy could not be totally ruled out. However, it is interesting to notice that our results are in excellent agreement with the room-temperature STM results of Kubby *et al.*,⁶ who observed local domains of asymmetric 2×1 , $c(4 \times 2)$, and $p(2 \times 2)$ structures in the same Ge(100) surface topographic image. Moreover, depending on both the amount of defects, the $c(4 \times 2)$ ordered phase can be broken into several domains with typical $p(2 \times 2)$ structure boundaries and the local $b(2 \times 1)$ areas corresponding to stronger disorder. Similarly, RT He diffraction experiments have also shown the existence of $c(4 \times 2)$ quarter order spots.¹⁴ It is likely that the amount of these different reconstructions depends on minor differences in surface preparation, as suggested by Kubby *et al.*⁶ However, it is not clear whether these results are compatible with a phase transition between the 2×1 and $c(4 \times 2)$ reconstructions, first predicted³³ and observed^{29,34,35} around 200–250 K and later calculated to be at another temperature range of 380 ± 100 K.⁹ In both LT and RT states, a mixing of at least two different reconstructions is likely to occur and may be consistent with a weak second order transition.

IV. CONCLUSIONS

We have performed *ab initio*, self-consistent molecular-cluster DMol calculations of the Ge(100) reconstructions. We have calculated total binding energy and equilibrium geometry up to the fourth layer of the symmetric 2×1 , asymmetric 2×1 , and $c(4 \times 2)$ reconstructions. Our results for the Ge(100) surface, which are in good agreement with a recent STM experiment, indicate important structural and energetic differences with the corresponding Si(100) surface. Asymmetric dimer reconstructions $b(2 \times 1)$ and $c(4 \times 2)$ result in a weakly bound Ge dimer, with bond lengths significantly larger than the bulk value and an up-dimer atom 0.2 Å above the ideal surface. This last feature might be of some relevance in the very different response of the Ge(100) surface [when compared to Si(100) one] observed upon adsorbate deposition. Also, the $b(2 \times 1)$ and $c(4 \times 2)$ reconstructions are found to be close in energy, well below the corresponding symmetric 2×1 reconstruction. This large energy difference between symmetric and asymmetric dimer models suggests that dynamical dimer flipping recently proposed for the Si(100) 2×1 surface is unlikely to take place at the Ge(100) surface.

ACKNOWLEDGMENTS

The work at Northwestern University was supported by the U.S. Office of Naval Research under Grant No. N00014-89J-1290 and by a computing grant of the U.S. Naval Oceanographic Office-Stennis Space Center and at Commissariat à l'Énergie Atomique by Ministère de l'Enseignement Supérieur et de la Recherche. The authors are grateful to S. P. Tang for collaboration and valuable discussions.

*Also at Department of Physics and Astronomy, Northwestern University, Evanston, Illinois 60208-3112.

¹J. P. Lafemina, Surf. Sci. Rep. **16**, 133 (1992).

²*Ordering at Surfaces and Interfaces*, edited by A. Yoshimori, T. Shinjo, and H. Watanabe, Springer Series in Materials Science Vol. 17 (Springer-Verlag, Berlin, 1990).

³J. A. Appelbaum and D. R. Hamann, Surf. Sci. **74**, 21 (1978).

⁴Z. Zhu, N. Shima, and M. Tsukada, Phys. Rev. B **40**, 11 868 (1989).

⁵S. P. Tang, A. J. Freeman, and B. Delley, Phys. Rev. B **45**, 1776 (1992), and references therein.

⁶J. A. Kubby, J. E. Griffith, R. S. Becker, and J. S. Vickers, Phys. Rev. B **36**, 6079 (1987).

⁷P. Krüger, A. Mazur, J. Pollmann, and G. Wolfgarten, Phys. Rev. Lett. **57**, 1468 (1986).

⁸M. Needels, M. C. Payne, and J. D. Joannopoulos, Phys. Rev. Lett. **58**, 1765 (1987).

⁹M. Needels, M. C. Payne, and J. D. Joannopoulos, Phys. Rev. B **38**, 5543 (1988).

¹⁰B. Goldstein, Surf. Sci. **35**, 227 (1973).

¹¹P. Soukiassian, T. Kendelewicz, and Z. D. Hurych, Phys. Rev. B **40**, 12 570 (1989).

¹²K. Hricovini, G. Lelay, A. Khan, A. Taleb-Ibrahimi, and J. E. Bonnet, in *Structure of Surfaces III*, edited by S. Y. Tong, X.

Xide, K. Tagayanaki, and M. A. Van Hove, Springer Series in Surface Science Vol. 24 (Springer-Verlag, Berlin, 1991), p. 589.

¹³K. M. Schirm, P. Soukiassian, Y. Borensztein, S. Nishigaki, G. S. Dong, K. Hricovini, and J. E. Bonnet, Appl. Surf. Sci. **68**, 433 (1993).

¹⁴W. R. Lambert, P. L. Trevor, M. J. Cardillo, A. Sakai, and D. R. Hamann, Phys. Rev. B **35**, 8055 (1987).

¹⁵J. Pollmann, P. Krüger, and A. Mazur, J. Vac. Sci. Technol. B **5**, 945 (1987).

¹⁶E. Landmark, R. I. G. Uhrberg, P. Krüger, and J. Pollmann, Surf. Sci. Lett. **236**, L359 (1990).

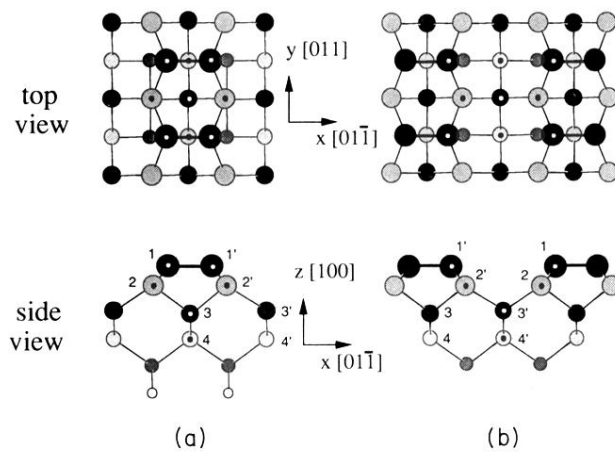
¹⁷R. Rossmann, H. L. Meyerheim, V. Jahns, J. Wever, W. Moritz, D. Wolf, D. Dornisch, and H. Schultz, Surf. Sci. **279**, 199 (1992).

¹⁸C. A. Lucas, C. S. Dower, D. F. McMorrow, G. C. L. Wong, F. J. Lamelas, and P. H. Fuoss, Phys. Rev. B **47**, 10 375 (1993).

¹⁹L. Ye, A. J. Freeman, and B. Delley, Phys. Rev. B **39**, 10 144 (1989); Surf. Sci. Lett. **239**, L526 (1990).

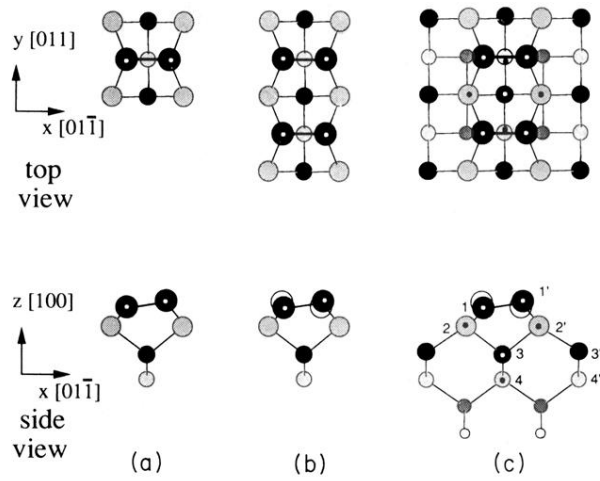
²⁰L. Spiess, P. S. Mangat, S. P. Tang, K. M. Schirm, A. J. Freeman, and P. Soukiassian, Surf. Sci. Lett. **289**, L631 (1993); P. S. Mangat, P. Soukiassian, K. M. Schirm, Z. Hurych, L. Spiess, S. P. Tang, A. J. Freeman, and B. Delley, Phys. Rev. B

- 47, 16 311 (1993).
- ²¹S. P. Tang and A. J. Freeman, *Phys. Rev. B* **47**, 1460 (1993).
- ²²R. E. Schlier and H. E. Farnsworth, *J. Chem. Phys.* **30**, 917 (1959).
- ²³R. M. Tromp, R. J. Hamers, and J. E. Demuth, *Phys. Rev. Lett.* **55**, 1303 (1985); *Phys. Rev. B* **34**, 5343 (1986).
- ²⁴A. Samsavar, E. S. Hirschorn, F. M. Leibsle, and T. C. Chiang, *Phys. Rev. Lett.* **63**, 2830 (1989).
- ²⁵J. A. Kubby, W. J. Greene, and P. Soukiassian, *J. Vac. Sci. Technol. B* **9**, 739 (1991).
- ²⁶M. Tsuda, T. Hoshino, S. Oikawa, and I. Ohdomari, *Phys. Rev. B* **44**, 11 241 (1991).
- ²⁷P. C. Weakliem, G. W. Smith, and E. A. Carter, *Surf. Sci. Lett.* **232**, L219 (1990).
- ²⁸R. A. Wolkow, *Phys. Rev. Lett.* **68**, 2636 (1992).
- ²⁹G. LeLay, J. Kanski, P. O. Nilsson, U. O. Karlsson, and K. Hricovini, *Phys. Rev. B* **45**, 6692 (1992).
- ³⁰M. Mitome and K. Tagayanaki, *Surf. Sci.* **242**, 69 (1991).
- ³¹J. Skov Pedersen, *Surf. Sci.* **210**, 238 (1989).
- ³²R. D. Schnell, F. J. Himpsel, A. Bogen, D. Rieger, and W. Steinmann, *Phys. Rev. B* **32**, 8052 (1985).
- ³³J. Ihm, D. H. Lee, J. D. Joannopoulos, and J. J. Xiong, *Phys. Rev. Lett.* **51**, 1872 (1983).
- ³⁴R. J. Culbertson, Y. Kuk, and L. C. Feldman, *Surf. Sci.* **167**, 127 (1986).
- ³⁵S. D. Kevan and N. G. Stoffel, *Phys. Rev. Lett.* **53**, 702 (1984); S. D. Kevan, *Phys. Rev. B* **32**, 2344 (1985).
- ³⁶B. Delley, *Chem. Phys.* **110**, 329 (1986); *J. Chem. Phys.* **92**, 508 (1990).
- ³⁷B. Delley, *J. Chem. Phys.* **94**, 7245 (1991).
- ³⁸DMol, Biosym Technologies Inc., San Diego, CA.
- ³⁹B. Delley, D. E. Ellis, and A. J. Freeman, *Phys. Rev. Lett.* **50**, 488 (1983).
- ⁴⁰X. Q. Wang, C. Z. Wang, B. L. Zhang, and K. M. Ho, *Phys. Rev. Lett.* **69**, 69 (1992).
- ⁴¹S. P. Tang and A. J. Freeman, *Phys. Rev. B* **47**, 2441 (1993).
- ⁴²L. Hedin and B. I. Lundqvist, *J. Phys. C* **4**, 2064 (1971).
- ⁴³E. Kaxiras and J. D. Joannopoulos, *Phys. Rev. B* **37**, 8842 (1988).



● — ⊙ center atoms mentioned in the text

FIG. 2. Clusters used for the investigation of the symmetric dimer reconstructed Ge(100) 2×1 surface. “Center atoms” used in the geometry optimization (step 1) are represented with a dot. (a) Ge₃₁-H₂₈ and (b) Ge₃₉-H₃₂. Hydrogen atoms are not represented for clarity.



○ position of back dimers from side view, for the $c(4 \times 2)$ structure

● — ⊙ center atoms mentioned in the text

FIG. 3. Clusters used for the investigation of the asymmetric dimer reconstructed Ge(100) surface. Center atoms used in the geometry optimization (step 1) are represented with a dot. (a) Ge9-H12, (b) Ge15-H16, and (c) Ge31-H28. Hydrogen atoms are not represented for clarity. Clusters (b) and (c) are used to study both the $b(2 \times 1)$ symmetry with parallel dimers and the $c(4 \times 2)$ reconstruction with alternating dimers as shown in the side view with empty spheres for the projection of background dimers. The small clusters (a) and (b) provide only qualitative results, useful in the investigation of cluster (c).

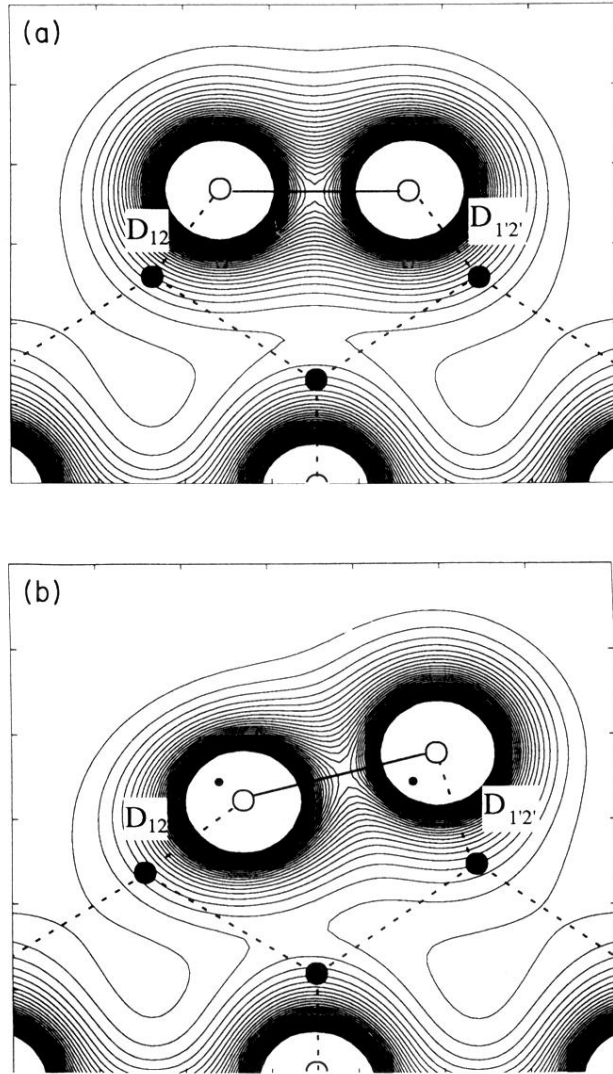


FIG. 5. Contour plot of the total charge density of the Ge(100)2×1 surface for (a) symmetric dimer and (b) the asymmetric dimer (positions of symmetric dimer atoms are recalled by small dots). The plots are in the (011) plane passing through the dimers and cutting the surface at a right angle. Contour spacings are 0.004 $e/(a.u.)^3$. Solid circles represent out-of-plane Ge atoms.